Chapter 2

Dielectric-Modulated TFETs as Label-Free Biosensors

Rupam Goswami and Brinda Bhowmick

Additional information is available at the end of the chapter

http://dx.doi.org/10.5772/intechopen.76000

Abstract

This chapter presents tunnel field effect transistors (TFETs) as dielectric-modulated (DM) label-free biosensors, and discusses various aspects related to them. A brief survey of the dielectric-modulated TFET biosensors is presented. The concept of dielectric modulation in TFETs is discussed with focus on principle and design perspectives. A Technology Computer Aided Design (TCAD) based approach to incorporate embedded nanogaps in TFET geometries along with appropriate physics-based simulation models are mentioned. Non-ideal conditions in dielectric-modulated biosensors are brought to light, keeping in view the practical considerations of the devices. A gate engineered TFET is taken up for analysis of sensitivities under different conditions through TCAD simulations. Finally, a status map of the sensitivities of the most significant works in dielectric-modulated label-free biosensors is depicted, and the status of the proposed TFET is highlighted.

Keywords: TFET, biosensor, dielectric modulation, biomolecules, sensitivity

1. Introduction

The dependence of economics of the semiconductor industry on Moore's Law led to the downscaling of device dimensions in metal oxide semiconductor field effect transistors (MOSFETs) in order to accommodate more transistors in the same chip area. As the device dimensions were scaled down to the nanometer regime, degradation in the performance of MOSFETs in the form of short channel effects (SCEs) was observed. The inversion charge sharing by the source and drain regions in short channel MOSFETs led to problems of drain induced barrier lowering (DIBL), threshold voltage roll-off, mobility degradation and high field saturation [1–3]. These problems hindered the progress of MOSFETs towards low power applications which required reduced supply voltage and targets of low off currents. Since

then, the semiconductor industry has been on the lookout for novel devices which can effectively address the issues of scaling and depict performance which is superior to MOSFETs.

Over the past few decades, industries and researchers have proposed a number of devices as prominent alternatives to MOSFETs for low power applications. Most of these devices possess principles of operation which are different from MOSFETs. The International Technology Roadmap for Semiconductors in its document 'Beyond CMOS' published in 2015 reported the emerging devices based on structure or materials and charge/non-charge entity [4]. This include a number of devices like nanowire FET [5–7], carbon nanotube FET [8–10], graphene FET [11–13], TFET [14–16], spin FET [17–19] and negative gate capacitance FET [20, 21]. Of these devices, TFETs have gained concentrated focus for low power applications due to their fundamental fabrication methodologies being similar to MOSFETs, and their ability to achieve sub-60 mV/dec subthreshold swing and lower off currents than MOSFETs. TFETs operate by interband tunneling mechanism unlike thermionic emission in MOSFETs due to which the high energy tails of the Fermi distribution of carriers while moving from source to drain get curtailed, resulting in low subthreshold swings and off currents. Different architectures of TFETs have been proposed till date to improve their performance and increase the on currents. [22, 23], nanowire TFET [24, 25], heterojunction TFET [26, 27], III-V TFET [28], triple material gate TFET [29, 30], cylindrical TFET [31] and SOI TFET [32] are some of the widely used structures.

TFETs have found their uses in a wide range of low power applications like digital circuits and memory applications [33–35]. However, recently, the emergence of FET-based biosensors has projected TFETs as biosensors based on dielectric modulation in which the dielectric constant along with the charge of the biomolecules in the gate dielectric region affect the drain current [36]. The sensitivity of the biosensor in presence of biomolecules is defined with respect to a reference value. A number of geometries of TFETs has been proposed as dielectric-modulated biosensors, and the analyses of their sensitivities having dependence on device parameters have been reported [37–41].

Section 2 of this chapter presents a brief report on the existing works on FET-based biosensors. In Section 3, the principle of dielectric modulation in TFETs and a reference architecture for TFETs as biosensors are discussed. Section 4 mentions the different physics-based models to be considered while simulating a TFET on a Technology Computer Aided Design (TCAD) tool. The different sensitivities are defined in Section 5. Section 6 mentions the various non-ideal conditions that may possibly exist in case of FET-based biosensors. A circular gate TFET is analyzed as a dielectric-modulated biosensor through TCAD simulation in Section 7. Section 8 concludes the chapter and comments on future scope.

2. A brief survey

The compactness, compatibility in fabrication and label-free detection have made FET-based biosensors one of the promising area of interests. Generally, there are two methods to detect the presence of biomolecules: gating effect and dielectric modulation. The gating effect uses

the gate dielectric material with receptors on its surface to immobilize the biomolecules [42]. Dielectric modulation, on the other hand, employs the effect of change in dielectric constant in a portion of the gate dielectric on the drain current and the associated electrical parameters [37–41]. The gating effect is effective for detecting charged biomolecules, while dielectric modulation can assist in sensing charged and neutral biomolecules.

Im et al. proposed a dielectric-modulated (DM) FET-based biosensor [36] after the ion sensitive FETs proposed in 1970s [43]. Sarkar and Banerjee presented a nanowire TFET in [42] demonstrating the gating effect for positively charged biomolecules. It is convenient to assume that the embedded nanogap is completely filled with biomolecules. However, Kim et al. reported on partially filled nanogaps in practical cases due to steric hindrance, and proposed a parameter, fill factor, defined as the percentage of the nanogap occupied by biomolecules [44]. Narang et al. provided similar simulation analyses for partially filled nanogaps for DM FET and PNPN TFET [11]. Narang et al. further presented a Poisson equation based analytical model to account for the effect of dielectric modulation in TFETs [38]. Partially filled nanogaps decrease the response of the biosensor, as the effective dielectric constant varies with position within the nanogap. Abdi and Kumar proposed the concept of deriving the sensitivity through ambipolar current in TFET [45]. Ahangari presented reports of a dual material gate nanowire junctionless TFET as a biosensor [46]. As the nanogap length increased, the sensitivity improved considerably. Kanungo et al. reported that a short gate dielectric-modulated TFET biosensor showed improved sensitivity than a full gate dielectric-modulated TFET [40].

3. Dielectric modulation in TFETs: concept and geometry

3.1. Principle of operation

A conventional homojunction TFET is a gated reverse-biased p-i-n structure [3]. As opposed to the thermionic emission in MOSFETs, the mechanism of transport in TFETs is band-to-band tunneling. In an n-TFET, when positive gate bias increases, the energy bands get suppressed as a result of which the width between the p + source valence band, and i-channel conduction bands reduces, thus facilitating the tunneling of electrons from the former to the latter as depicted in **Figure 1** [3]. This contributes to the drain current.

The tunnel barrier at the source-channel junction is modeled as a triangular barrier, and using WKB approximation, its tunneling probability is calculated as [47].

$$T(E) = exp\left(-\frac{4\lambda\sqrt{2\,m^{*}\,E_G^{3/2}}}{3q\hbar\left(\Delta\Phi + E_G\right)}\right) \tag{1}$$

where m* is the effective mass, E_G is the energy band gap at the source-channel tunnel junction, $\Delta\Phi$ is the energy overlap of the bands at tunnel junction, λ is the screening tunneling length, q is the electronic charge, and $\hbar$ is the reduced Planck's constant. The screening length λ is defined as [47].

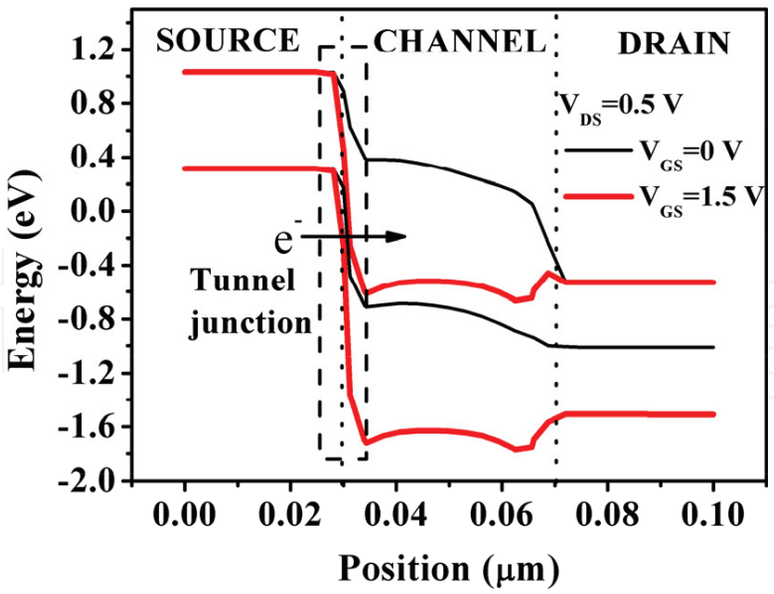

Figure 1. Energy band diagram of a p-i-n TFET showing the on and off states.

$$\lambda = \sqrt{(\varepsilon_s/\varepsilon_{ox})\, t_s\, t_{ox}} \tag{2}$$

The dielectric modulation in a MOS-based device, and particularly TFETs is the alteration in the dielectric constant in the gate dielectric region of the device. Keeping other parameters constant, the effect of dielectric modulation in TFET is best explained by the parameters, λ and $\Delta\Phi$. A low dielectric constant decreases the gate-to-channel coupling as a result of which the tunnel width is more even at high gate voltages, as compared to the presence of higher gate dielectric constants at the tunnel junction [3, 47, 48]. This results in a low tunneling probability, and hence, low tunneling current. Lesser the gate-to-channel coupling, lesser is the amount of $\Delta\Phi$ at the tunnel junction.

A 2-D Poisson's equation based model of TFET results in a closed form equation of drain current as [49].

$$I_{DS} = W\, T_{Si,eff}\, \frac{E_G}{W_{t,min}^2} \cdot \frac{A_K}{B_K} . exp\left(-\frac{B_K E_G}{q\, W_{t,min}}\right) \tag{3}$$

where, W is the width of the device, $T_{Si,eff}$ is the effective Silicon body thickness, E_G is the band gap of the semiconductor, $W_{t,min}$ is the minimum tunneling width, A_K and B_K are material dependent constants. Equation (3) suggests the dependence of drain current on the minimum tunnel width which, in turn, is dependent on the dielectric constant of the gate insulator region near the tunnel junction. Therefore, as dielectric constant of the nanogap increases, $W_{T,min}$ decreases, and drain current increases.

Another prospect of utilizing dielectric modulation for biosensing is by placing the embedded nanogap towards the channel-drain junction of the TFET, and exploit its ambipolarity [45]. For a conventional n-TFET, when the drain voltage is positive, and gate voltage is negative,

the energy bands at the channel-drain junction get influenced so as to form a tunneling barrier. This results in flow of current by tunneling at this junction. This becomes the reason for anomalies in complementary TFET digital circuits. However, as far as label-free biosensing is concerned, this ambipolar current can be considered as a measure of sensitivity in TFETs.

3.2. Geometry

As evident from Section 3.1, the objective of utilizing dielectric modulation for biosensing requires a modified geometry with the following basic requirements

- The biomolecules must be immobilized in the gate dielectric region. To realize this, a nanogap is required in the gate dielectric. The gate dielectric, therefore, is composed of two regions; apparently, it works like a dual gate dielectric device, where one gate dielectric has a fixed dielectric constant, and the other carries the dielectric constant of the biomolecules.
- The height of the embedded nanogap must be large enough to allow the entry of biomolecules into the cavity or nanogap. A minimum height of 10–11 nm is usually considered for simulation analyses in nanoscale TFETs.
- In order to accommodate more biomolecules, a double gate structure with the above designs may be employed.
- The TFETs must have appropriate source doping. A few biomolecules have dielectric constants of 2 or 3 [39–42], which is closer to the dielectric constant of 1. So, the geometry must be so designed that it is able to respond to immobilization of biomolecules having low dielectric constants as well.
- For TFETs which utilize the ambipolar behavior of the devices, the drain doping concentration is more important.

4. Simulation strategy for a DM TFET as a label-free biosensor

The most convenient way to analyze a biosensor is on a computational platform where the physics-based models applied to the architecture assist in analyzing its performance. There are a number of industrial simulators and most of them come equipped with provisions for defining a geometry and feeding it through iterations of selective models available in their libraries.

The embedded nanogap in a DM TFET is designed by substituting that region in the gate dielectric with a dielectric material (oxide) whose dielectric constant can be altered as per requirement [38]. For charged biomolecules, the charges are considered at the oxide-semiconductor interface. By varying the dielectric constant and the charge, the immobilization of biomolecules may be mimicked appropriately.

The models for TFETs must be chosen with care. Since TFETs usually have high source doping concentration to achieve large band bending at equilibrium, therefore, Fermi-Dirac statistics

is necessary [50]. Bandgap narrowing is important for heavily doped geometries [50]. Nonlocal band-to-band tunneling models are essential to create a suitable simulation environment for the device whose principle of operation is interband tunneling [50]. Field dependent mobility models may be used [50].

5. Sensitivity parameters

The performance of a TFET or any MOS-based device is reflected through its electrical parameters. The most commonly used parameters for defining sensitivity are the drain current and threshold voltage. Subthreshold swing (SS) may also be considered for defining a sensitivity parameter; however, the measurement of SS is dependent on the orders of the logarithmic scale over which the drain current is measured. This value or the measurement may not be consistent as the drain current changes with the variation in the dielectric constant of the immobilized biomolecules. Sensitivities are usually defined with respect to reference values. The reference value in case of a dielectric-modulated biosensor is considered when the nanogap is devoid of biomolecules, and hence, is assumed to be filled with air with a dielectric constant of 1 without any charges at the oxide-semiconductor interface. The drain current based sensitivity is mathematically expressed as [44].

$$Sensitivity,\ S_I = \left.\frac{I_{D,k}}{I_{D,k=1}}\right|_{V_{GS}} \tag{4}$$

where $I_{D,k}$ and $I_{D,k=1}$ are the values of drain currents when the nanogap is filled with biomolecules and the nanogap is unfilled. The values must be measured at the same gate voltage so as to get a justified value of sensitivity.

The threshold voltage has a dependence on the dielectric constant of the gate dielectric and charge at the semiconductor-oxide interface. The shift in threshold voltage with the immobilization of biomolecules with different dielectric constants may be taken up as a sensitivity parameter. It is mathematically expressed as

$$Sensitivity,\ S_{V_T} = V_{T,k=1} - V_{T,k} \tag{5}$$

where $V_{T,k}$ and $V_{T,k=1}$ are the threshold voltages for the cases when the nanogap is filled with biomolecules and when the nanogap is completely unfilled.

There are many threshold voltage extraction methods for MOSFETs, and TFETs. Of them, the Linear Extrapolation (LE) Method is the most widely used [51, 52]. According to this extraction principle, the intercept on the gate voltage axis made by the tangent to the drain current curve corresponding to the maximum value of $g_m = dI_D/dV_{GS}$ is defined as the threshold voltage. Although this extraction method may result in change in threshold voltage with change in range in gate voltage, however, we have considered a fixed range of gate voltage in all the cases of comparison. So, we have used this method of threshold voltage extraction from simulation transfer characteristics.

6. Non-idealities in dielectric-modulated biosensors

While simulating a geometry of a DM TFET as on a TCAD tool to assess its biosensing capacity, it is convenient to assume that the nanocavity is completely filled with the biomolecules. However, in practical cases, the issues of steric hindrance and probe placement do not allow the embedded nanogap to be completely filled [39]. As a result, partially filled nanogaps are formed.

6.1. Steric hindrance

In case of steric hindrance, the biomolecules which get immobilized first prevent the further entry of biomolecules. In fact, there is a hindrance to the biomolecules which are likely to get immobilized in the nanogaps, resulting in partial hybridization. In order to account for this on a TCAD tool for simulation, different patterns of immobilization inside the nanogap are assumed, like increasing, decreasing, concave and convex profiles of placement [39]. As explained in Section 2, this can be designed by defining different heights of gate dielectric material mimicking the biomolecules according to the profile of biomolecules.

6.2. Probe placement

In order to immobilize the biomolecules, probes or receptors are used in the nanogap. The placement of probes in the nanogap for immobilization of biomolecules may not be continuous throughout, and this may result in partially filled nanogaps [39]. For simulation, this may be considered in a similar manner as the steric hindrance except that the profiles shall not be continuous as in steric hindrance.

6.3. Fabrication issues

The nanogap which is formed in a DM biosensor is carved out by forming a native oxide first, and then etching out the native oxide [38]. This method, however, is challenging, and practically, there is possibility that damages result from the process. These anomalies include creation of trap centers at the interface or incomplete etch of the native oxide along with traps in the residual gate dielectric [38]. The phenomenon of tunneling in a TFET is highly dependent on its source-channel tunnel junction, and the alignment of the gate with the junction. During fabrication, the gate edge may be displaced from the junction. This may result in an overlap or an underlap depending on whether the gate shifts towards the source or the channel respectively. In case of a gate-source overlap, the characteristics of the TFET generally improve as the shifted gate can now influence the energy bands in the source-channel junction with better control. However, in case of an underlap, the gate edge moves away from the junction, and the tunnel junction is least affected by it.

7. A circular gate TFET as a DM biosensor

This section presents a geometry of TFET, a Circular Gate TFET (CG) as a dielectric-modulated biosensor, and discusses some of the results. The CG TFET has a non-uniform gate in the

form of a semi-circle. This gate engineering introduces flexibility into the architecture of the device, and aids in optimization of chief electrical parameters, primarily the ambipolar current and ratio of on and off currents [53]. One of the techniques of reducing ambipolar current in a TFET apart from asymmetric source-drain doping is the introduction of gate-drain underlap [3, 45, 53]. In case of Circular Gate TFET, the gate being circular in shape, the gate dielectric thickness is dependent on the radius of the circle. A gate-drain underlap in the architecture shall decrease the thickness of the gate dielectric, which shall, in turn, increase the influence of the gate on the channel. Therefore, reduced ambipolar current can be achieved with appropriate ratio of on and off current simultaneously.

A circular gate TFET as a DM biosensor is depicted in **Figure 2a**. The total length of the Silicon body TFET is 100 nm, where the source and drain are 30 nm each. An embedded nanogap is incorporated into the geometry to immobilize the biomolecules. The embedded nanogap is usually etched out of a dielectric formed by a native oxide. We have considered a native oxide of 1 nm in the nanogap, which is assumed to remain after the gap is etched out.

7.1. Fully filled nanogap

Firstly, we assume that the entire embedded nanogap of the CG TFET in **Figure 2b** is filled with biomolecules, and observe the influence of different factors on its sensitivity. The Fill Factor of an embedded nanogap is defined as the ratio of the area covered by immobilized biomolecules to the total area of the nanogap, and is generally expressed in percentage. For a fully filled nanogap, the Fill Factor is 100%.

7.1.1. Negatively charged biomolecules

The sensitivity of the CG TFET as a biosensor with fully filled nanogap is plotted for negative charge of biomolecules for k = 5, 7, 10 and 12 in **Figure 3a**. With the increase in magnitude of negative charge, the sensitivity decreases. The presence of negatively charged biomolecule-SiO_2 interface prevents depletion of the p-type channel, thus requiring a higher gate voltage than a neutral interface to deplete the p-type substrate, and cause reduction in tunnel width. The voltage balance equation of a metal-oxide-semiconductor structure is represented as [54].

$$V_G = \psi_s + \Phi_{MS} - \frac{q N_{bio}}{C'_{ox}} \tag{6}$$

where, V_G is the gate voltage, Ψ_s is the electrostatic potential at the surface, Φ_{MS} is the difference between the work functions of metal and semiconductor, q is the value of electronic charge, N_{bio} denotes the number of charges per unit area, and C'_{ox} is resultant capacitance per unit area. Furthermore,

$$C'_{ox} = \frac{k}{t_{ox}(x)} \tag{7}$$

where k is the dielectric constant, and $t_{ox}(x)$ is the dielectric thickness as a function of lateral position due to the circular gate.

http://dx.doi.org/10.5772/intechopen.76000

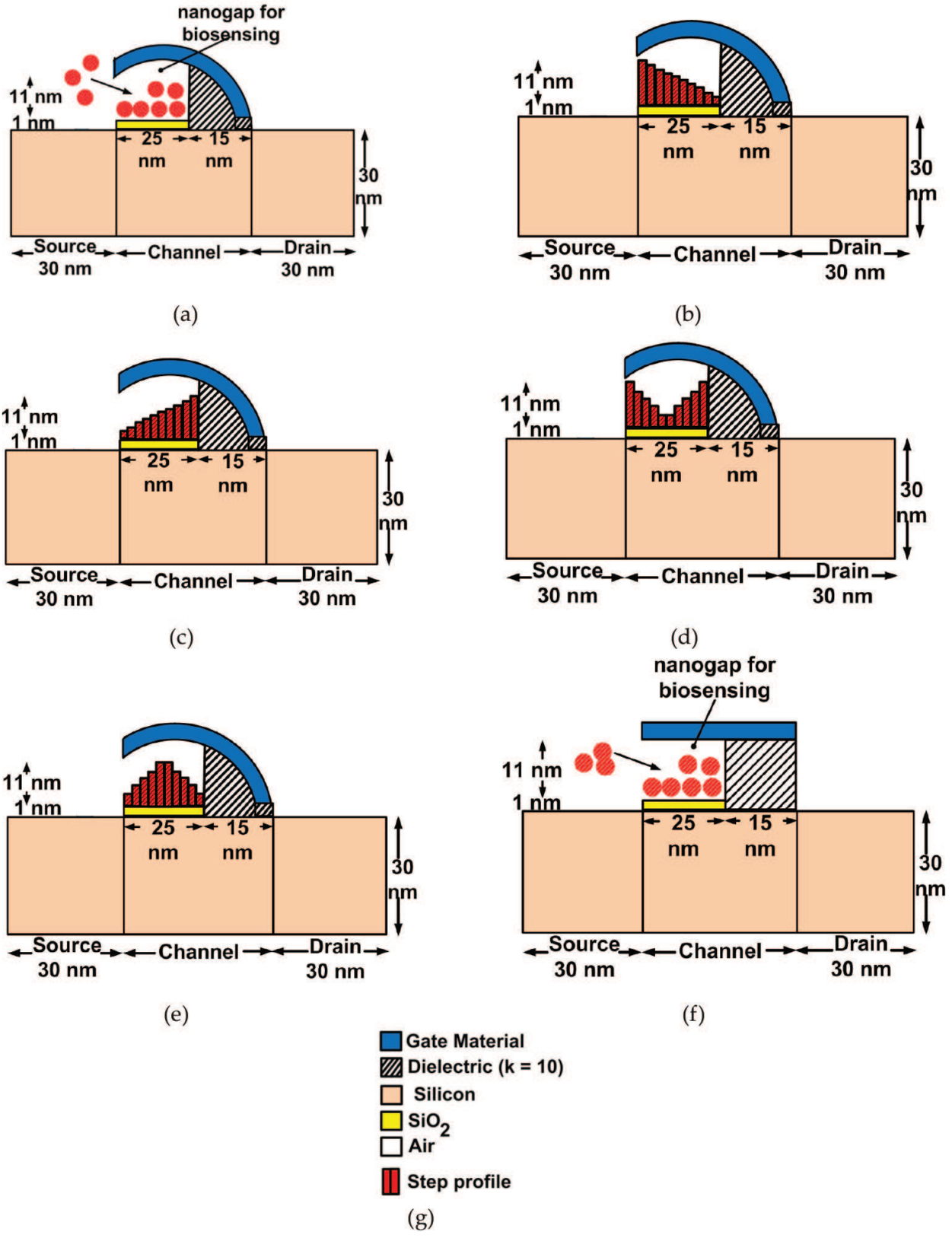

Figure 2. 2-D schematic of dielectric-modulated biosensors: (a) CG TFET, (b) decreasing step profile of biomolecules, (c) increasing step profile of biomolecules, (d) concave step profile of biomolecules, (e) convex step profile of biomolecules, (f) MOSFET, and (g) legend for all the 2D schematics.

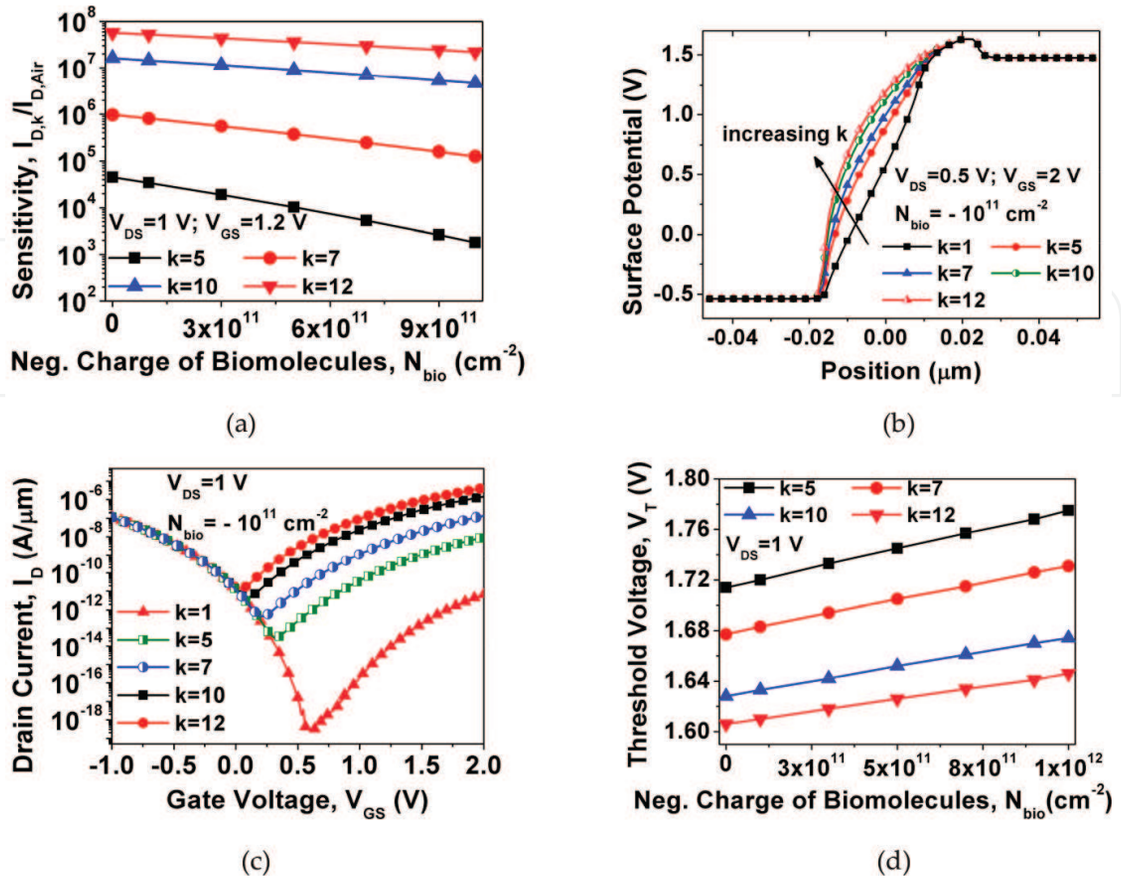

Figure 3. (a) Sensitivity versus negative charge of biomolecules for dielectric constant, k = 5, 7, 10 and 12; (b) surface potential versus position from source to drain at gate voltage 2 V, drain voltage 0.5 V, and $N_{bio} = -10^{11}$ cm^{-2} for dielectric constant, k = 1, 5, 7, 10 and 12; (c) transfer characteristics of CG TFET as biosensor for k = 1 (air), 5, 7, 10 and 12 at fixed negative charge, $N_{bio} = -10^{11}$ cm^{-2}; (d) threshold voltage versus negative charge of biomolecules for dielectric constant, k = 5, 7, 10 and 12.

Considering a fixed gate voltage, as the negative charge of biomolecules increases, Ψ_s must decrease in order to satisfy the potential balance in Eq. (6). As a result, the drain current decreases, thus reducing the sensitivity.

The change in sensitivity of the sensor with increasing magnitude of negative charge is more in case of a low dielectric constant and reduces as the dielectric constant of the nanogap increases. At k = 5, the sensitivity decreases by a factor of 25 when the charge of the immobilized biomolecules changes from neutral to -10^{12} cm^{-2} as compared to k = 12, where it drops by 2.61. In Eq. (6), at fixed negative N_{bio} and V_{GS}, as k in Eq. (7) increases, the potential $-\frac{q N_{bio}}{C'_{ox}}$ decreases, resulting in a corresponding increase in Ψ_s. This increases the drain current, and hence, the sensitivity of the biosensor. This effect is demonstrated in **Figure 3b**.

Figure 3c shows the plots of transfer characteristics of a fully filled nanogap CG TFET biosensor at drain voltage 1 V and charge of biomolecules equal to -10^{11} cm^{-2}. The absence of biomolecules corresponds to k = 1 with no charge at the air-SiO_2 interface as the nanogap remains devoid of biomolecules. Due to the presence of unaltered gate dielectric towards the channel-drain junction of the geometry, therefore, the ambipolar current is same for all dielectric constants of the nanogap. The dielectric constant of the fully filled nanogap closer to the

source-channel tunnel junction has an impact on the drain current. However, as the dielectric constant increases, the minimum value of drain current shifts to the left, thus, verifying the increase in gate capacitance. This corresponds to a decrease in the threshold voltage as shown in **Figure 3d**. The threshold voltage exhibits a high shift with increasing negative charge for low-*k* biomolecules as compared to high-*k* cases. For $k = 5$, the threshold voltage increases by 3.56% as the charge of the immobilized biomolecules change from neutral to -10^{12} cm^{-2} as compared to $k = 12$ where the increase is relatively small, that is, 2.49%.

7.1.2. Positively charged biomolecules

Like Section 7.1.1, similar plots are presented here for positive charge of biomolecules. The variation of sensitivity with increasing positive charges for $k = 5$, 7, 10 and 12 is shown in **Figure 4a**. The positive charge of biomolecules depletes the p-type channel, and causes more tunneling of electrons at the source-channel tunnel junction. Hence, the sensitivity increases. For $k = 5$, the sensitivity increases by a factor of 11 when the charge changes from neutral to 10^{12} cm^{-2}, whereas for $k = 12$, the factor is 2.29. The explanation for the trend of the plot can be made in a similar manner as in Section 7.1.1 with the help of Eqs. (6) and (7).

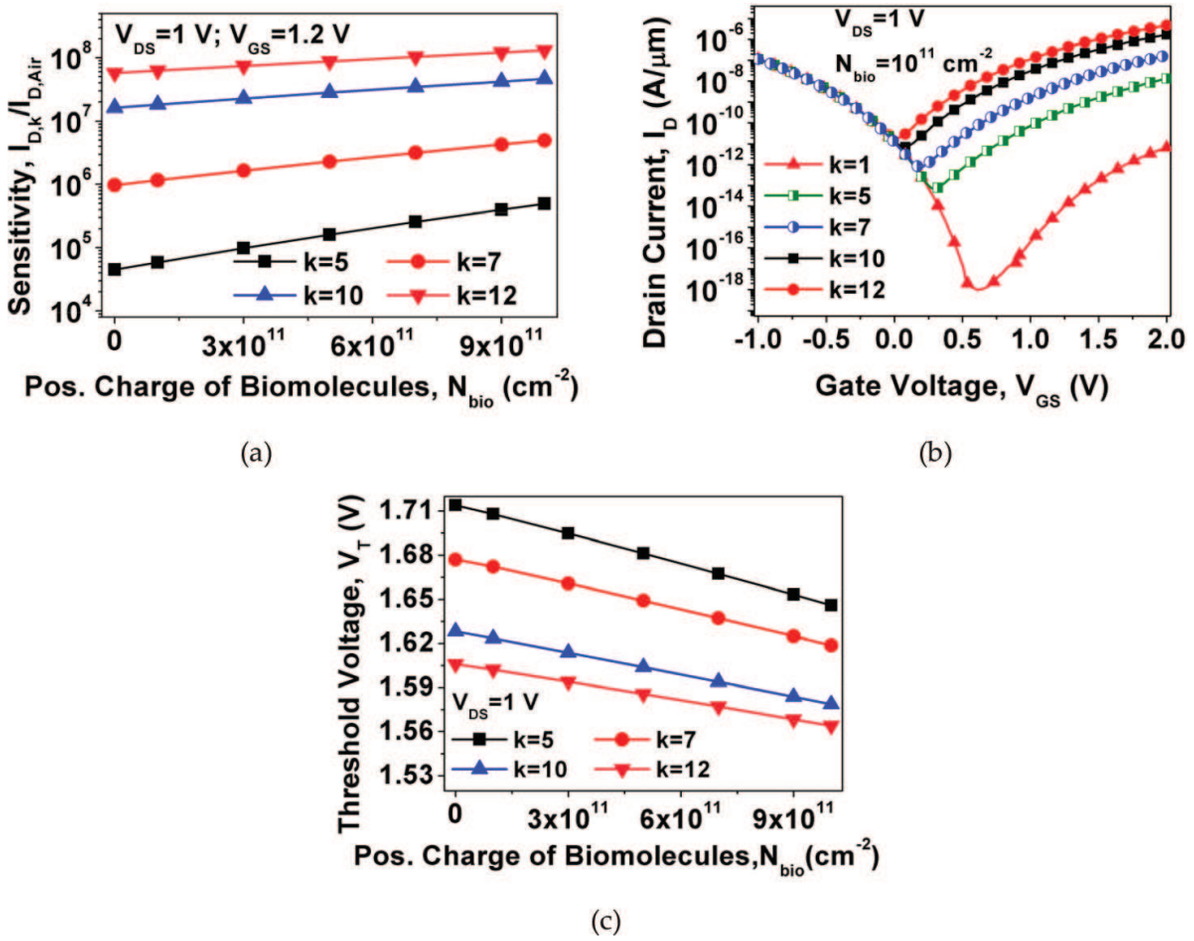

Figure 4. (a) Sensitivity versus positive charge of biomolecules for dielectric constant, $k = 5$, 7, 10 and 12; (b) transfer characteristics of CG TFET as biosensor for $k = 1$ (air), 5, 7, 10 and 12 at fixed negative charge, $N_{bio} = 10^{11}$ cm^{-2}; (c) threshold voltage versus positive charge of biomolecules for dielectric constant, $k = 5$, 7, 10 and 12.

Figure 4b depicts the transfer characteristics of the CG TFET for k = 5, 7, 10, and 12 at $N_{bio} = 10^{11}$ cm^{-2}. The on current in case of positive charged biomolecules is higher than that in case of negatively charged biomolecules as evident from **Table 1**.

In **Figure 4c**, for k = 5, the threshold voltage decreases by 4.03% when the charge changes from neutral to 10^{12} cm^{-2}, whereas for k = 12, the drop is 2.68%.

7.1.3. Sensitivities of DM CG TFET and MOSFET

The comparisons of sensitivities of CG TFET and MOSFET are shown in **Figure 5a** and **b**. At $N_{bio} = \pm 5 \times 10^{11}$ cm^{-2}, the values are extracted for k = 5, 7, 10, and 12. The MOSFET with exactly equal nanogap height and length as that of CG TFET exhibits extremely inferior sensitivity as compared to CG TFET. Earlier works on dielectric-modulated MOSFET have reported similar poor sensitivity of the device as compared to TFET [38, 39].

Sl. No. (horizontal axis of Figure 7)	**Biosensors**	**Reference**
1	Conventional FET	[42]
2	Nanowire TFET	
3	DM FET (L_{GAP} = 200 nm, H_{GAP} = 15 nm, k = 2.1)	[36]
4	DM FET (L_{GAP} = 100 nm, H_{GAP} = 15 nm, k = 2.1)	
5	Full Gate DMTFET (L_{GAP} = 10 nm, L_{GATE} = 42 nm, H_{GAP} = 5 nm, k = 4)	[40]
6	Short Gate DMTFET (L_{GAP} = 10 nm, L_{GATE} = 20 nm, H_{GAP} = 5 nm, k = 4)	
7	DM FET (L_{GAP} = 30 nm, L_{GATE} = 100 nm, H_{GAP} = 9 nm, k = 10)	[39]
8	DM FET (L_{GAP} = 75 nm, L_{GATE} = 250 nm, H_{GAP} = 9 nm, k = 10)	
9	DM PNPN TFET (L_{GAP} = 30 nm, L_{GATE} = 100 nm, H_{GAP} = 9 nm, k = 10)	
10	DM PNPN TFET (L_{GAP} = 75 nm, L_{GATE} = 250 nm, H_{GAP} = 9 nm, k = 10)	
11	DM STS I-MOS (L_{GAP} = 50 nm, L_{GATE} = 120 nm, H_{GAP} = 15 nm, k = 10)	[55]
12	SiGe Source DM PNPN TFET, Ge composition = 0% (L_{GAP} = 15 nm, L_{GATE} = 100 nm, H_{GAP} = 9 nm, k = 2.1)	
13	SiGe Source DM PNPN TFET, Ge composition = 10% (L_{GAP} = 15 nm, L_{GATE} = 100 nm, H_{GAP} = 9 nm, k = 2.1)	[41]
14	SiGe Source DM PNPN TFET, Ge composition = 20% (L_{GAP} = 15 nm, L_{GATE} = 100 nm, H_{GAP} = 9 nm, k = 2.1)	
15	CG TFET (L_{GAP} = 25 nm, L_{GATE} = 40 nm, H_{GAP} = 11 nm, k = 10)	Proposed Work
16	CG TFET (decreasing step) (L_{GAP} = 25 nm, L_{GATE} = 40 nm, H_{GAP} = 11 nm, k = 10)	
17	CG TFET (concave step) (L_{GAP} = 25 nm, L_{GATE} = 40 nm, H_{GAP} = 11 nm, k = 10)	

Table 1. Different reported works on biosensors numbered along the horizontal axis of **Figure 7**.

http://dx.doi.org/10.5772/intechopen.76000

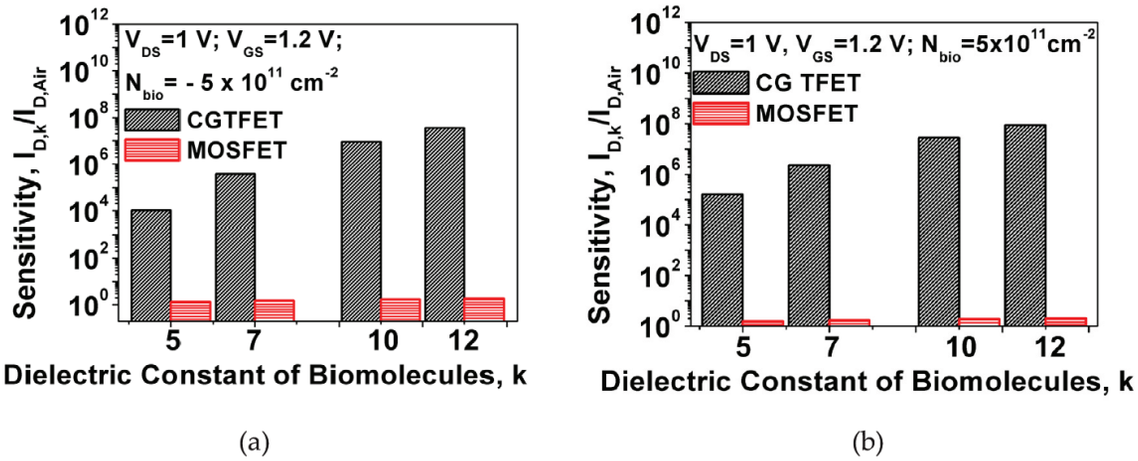

Figure 5. (a) Comparison of sensitivities of dielectric-modulated CG TFET and MOSFET biosensors at gate voltage 1.2 V, drain voltage 1 V and $N_{bio} = -5 \times 10^{11}$ cm^{-2} for dielectric constant, k = 5, 7, 10 and 12; (b) comparison of sensitivities of dielectric-modulated CG TFET and MOSFET biosensors at gate voltage 1.2 V, drain voltage 1 V and $N_{bio} = 5 \times 10^{11}$ cm^{-2} for dielectric constant, k = 5, 7, 10 and 12.

Not only does a shorter channel length affect the electrical characteristics of a MOSFET, but also its principle of thermionic emission by which its operation contributes to such low sensitivity. On the contrary, TFETs which operate by band-to-band tunneling perform well even when scaled. This advantage of TFET is suitable to be exploited for its biosensing capabilities.

7.2. Partially filled Nanogap

The comparison of sensitivity for the four different profiles of partially filled nanogap shown in **Figure 1b–e** is shown in **Figure 6**. Only the decreasing and concave step profiles of biomolecule immobilization respond well to the change in dielectric constant. Contrary to this, the

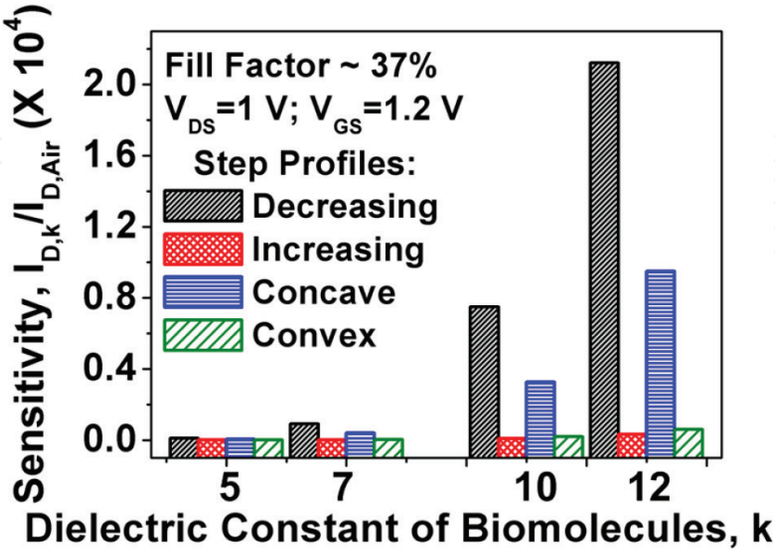

Figure 6. Comparison of sensitivities of step profiles of partially filled nanogap in CG TFET biosensor for dielectric constant, k = 5, 7, 10 and 12.

increasing and convex step profiles demonstrate poor sensitivity. The reason for this is the proximity of the highest step with the source-channel tunnel junction. In case of decreasing and concave step profiles, the higher steps are present near to the tunnel junction as shown in **Figure 1b**, **d** respectively. As the value of k increases, the gate-channel coupling increases in the region of higher steps closer to the tunnel junction. So, the response of the biosensor is better than that of the increasing and convex step profiles where the higher steps are located away from the source-channel tunnel junction.

7.3. Status map of biosensors

There are a number of important simulated and modeled works reported on dielectric-modulated TFET and FET. This section presents a map of the sensitivities of such biosensors proposed till date along with sensitivity of the proposed CG TFET.

Although the status map of **Figure 7** mentions the maximum or best sensitivities of each work, yet the architectural specifications under which the biosensors have been reported vary from one to another, and hence, drawing comparisons among them through **Figure 7** is not justified. However, there are a few conclusions that can be derived from the status map. Dielectric-modulated TFETs are more sensitive to the presence of biomolecules than MOSFETs due to the difference in their current transport mechanisms. In MOSFETs, sensitivities reduce at lesser channel lengths. The CG TFET, with a channel length of 40 nm, shows significant sensitivity; a fully filled nanogap in CG TFET for k = 10 has sensitivity closer to that of DM PNPN TFET for k = 10 possessing a channel length of 250 nm and nanogap length of 75 nm. However, the partially filled nanogaps (decreasing and concave step profiles) have lesser sensitivities than the fully filled case as explained in Section 7.2.

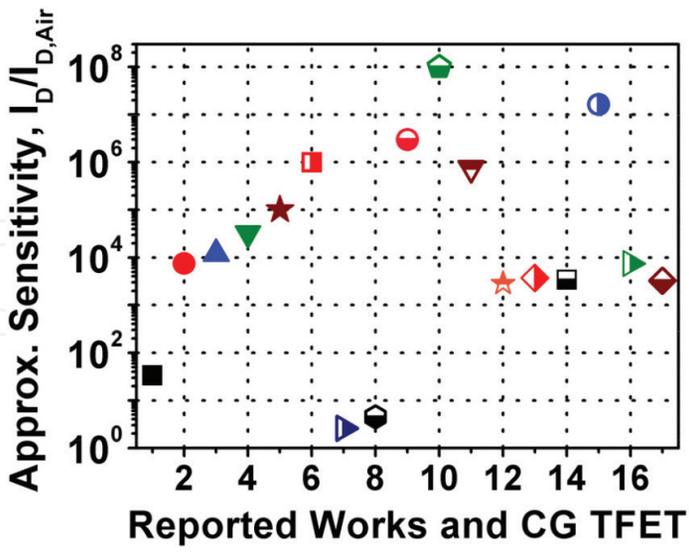

Figure 7. Sensitivities of FET-based biosensors of reported works and those of CG TFET. The sensitivities are extracted from the published works, and due to the possible tolerances in extraction, the vertical axis is named as 'approximate sensitivity'. The various biosensors are referred by using serial numbers from 1 to 17, the details of which are listed in **Table 1**.

8. Conclusion

This chapter has presented an overview on Tunnel Field Effect Transistors (TFETs) as dielectric-modulated biosensors. Tunnel Field Effect Transistors have emerged as one of the most significant devices for low power applications due to their ability to withstand the effects of scaling. With the interests gathering around FET-based biosensors, research on TFETs as biosensors has recently brought new focus. This chapter has discussed the various aspects of dielectric-modulated TFET as biosensor with emphasis on the design and development through simulation analyses. Practical implications of the biosensors are presented. A Circular Gate TFET as a dielectric-modulated biosensor is presented and analyzed at lesser channel length. The CG TFET is observed to offer an impressive sensitivity as compared to other biosensors. The different challenges in implementing a TFET-based dielectric-modulated biosensor are varied, ranging from the problems of steric hindrance, fabrication issues and uncertainty of probe placement. Simulation and modeling may enable one to predict the various effects. Appropriate physics-based models are necessary to validate the results on TCAD tool.

Author details

Rupam Goswami[1]* and Brinda Bhowmick[2]

*Address all correspondence to: rupam.goswamifet@kiit.ac.in

1 Kalinga Institute of Industrial Technology, Bhubaneswar, India

2 National Institute of Technology Silchar, Silchar, India

References

[1] Sarangi S, Bhushan S, Santra A, Dubey S, Jit S, Tiwari PK. A rigorous simulation based study of gate misalignment effects in gate engineered double-gate (DG) MOSFETs. Superlattices and Microstructures. 2013;**60**:263-279. DOI: 10.1016/j.spmi.2013.05.009

[2] Choi WY, Park B-G, Lee JD, Liu T-JK. Tunneling field-effect transistors (TFETs) with subthreshold swing (SS) less than 60 mV/dec. IEEE Electron Device Letters. 2007;**28**(8):743-745. DOI: 10.1109/led.2007.901273

[3] Royer CL, Mayer F. Exhaustive experimental study of tunnel field effect transistors (TFETs): From materials to architecture. In: 10th International Conference on Ultimate Integration of Silicon; March 18-20, 2009. Aachen: IEEE; 2009. pp. 53-56. DOI: 10.1109/ulis.2009.4897537

[4] International Technology Roadmap for Semiconductors. http://public.itrs.net/. 2015 Edition. [Accessed: January 06, 2018]

[5] Yang F-L et al. 5nm-gate nanowire fin FET. In: Digest of Technical Papers Symposium. VLSIT; June 15-17, 2004. Honolulu: IEEE; 2004. pp. 196-197. DOI:10.1109/VLSIT.2004.1345476

[6] Elmessary MA, Nagy D, Aldegunde M, Seoane N, Indalecio G, Lindberg J, et al. Scaling/LER study of Si GAA nanowire FET using 3D finite element Monte Carlo simulations. Joint International EUROSOI Workshop and International Conference on Ultimate Integration on Silicon (EUROSOI-ULIS), January 25-27, 2016. Vienna: IEEE; 2016. pp. 52-55. DOI: 10.1109/ulis.2016.7440050

[7] Yoon J-S, Kim K, Rim T, Baek C-K. Performance and variations induced by single interface trap of nanowire FETs at 7-nm node. IEEE Transactions on Electron Devices. 2017;**64**(2): 339-345. DOI: 10.1109/ted.2016.2633970

[8] Wong HSP. Beyond the conventional transistor. IBM Journal of Research and Development. 2002;**46**(2.3):133-168. DOI: 10.1147/rd.462.0133

[9] Guo J, Datta S, Lundstrom M. A numerical study of scaling issues for Schottky-barrier carbon nanotube transistors. IEEE Transactions on Electron Devices. 2004;**51**(2):172-177. DOI: 10.1109/ted.2003.821883

[10] Yousefi R, Shabani M. A model for carbon nanotube FETs in the ballistic limit. Microelectronics Journal. 2011;**42**(11):1299-1304. DOI: 10.1016/j.mejo.2011.08.012

[11] Fiori G, Iannaccone G. Simulation of graphene nanoribbon field-effect transistors. IEEE Electron Device Letters. 2007;**28**(8):760-762. DOI: 10.1109/led.2007.901680

[12] Echtermeyer T, Lemme M, Baus M, Szafranek B, Geim A, Kurz H. Nonvolatile switching in graphene field-effect devices. IEEE Electron Device Letters. 2008;**29**(8):952-954. DOI: 10.1109/led.2008.2001179

[13] Tamersit K, Djeffal F. Double-gate graphene Nanoribbon field-effect transistor for DNA and gas sensing applications: Simulation study and sensitivity analysis. IEEE Sensors Journal. 2016;**16**(11):4180-4191. DOI: 10.1109/jsen.2016.2550492

[14] Nirschl T, Wang P-F, Hansch W, Schmitt-Landsiedel D. The tunnelling field effect transistors (TFET): The temperature dependence, the simulation model, and its application. In: IEEE International Symposium on Circuits and Systems; May 23-26, 2004. Vancouver: IEEE, p. III-713-16. DOI: 10.1109/ISCAS.2004.1328846

[15] Jiang C, Liang R, Xu J. Investigation of negative capacitance gate-all-around tunnel FETs combining numerical simulation and analytical modeling. IEEE Transactions on Nanotechnology. 2016;**16**(1):58-67. DOI: 10.1109/tnano.2016.2627808

[16] Omura Y, Mallik A, Matsuo N. The impact of a fringing field on the device performance of a P-channel tunnel field-effect transistor with a high-κ gate dielectric. In: MOS Devices for Low-Voltage and Low-Energy Applications. Singapore: Wiley; 2016. pp. 399-411. DOI: 10.1002/9781119107361.ch34

[17] Shen M, Saikin S, Cheng M-C. Spin injection in spin FETs using a step-doping profile. IEEE Transactions On Nanotechnology. 2005;**4**(1):40-44. DOI: 10.1109/tnano.2004.840150

[18] Datta S, Das B. Electronic analog of the electro-optic modulator. Applied Physics Letters. 1998;**56**(7):665-667. DOI: 10.1063/1.102730

[19] Sugahara S, Tanaka M. A spin metal-oxide-semiconductor field-effect transistor (spin MOSFET) with a ferromagnetic semiconductor for the channel. Journal of Applied Physics. 2005;**97**(10):10D503. DOI: 10.1063/1.1852280

[20] Salahuddin S. Review of negative capacitance transistors. In: International Symposium on VLSI Technology, Systems and Application (VLSI-TSA); April 25-27, 2016. Hsinchu: IEEE. pp. 1-1. DOI: 10.1109/vlsi-tsa.2016.7480491

[21] Jo J, Shin C. Impact of temperature on negative capacitance field-effect transistor. Electronics Letters. 2015;**51**(1):106-108. DOI: 10.1049/el.2014.3515

[22] Boucart K, Ionescu A. Double gate tunnel FET with ultrathin silicon body and high-k gate dielectric. In: Proceedings of the European Solid-State Device Research Conference, September 19-21, 2006. Montreux: IEEE; 2007. pp. 1725-1733. DOI: 10.1109/essder.2006.307718

[23] Boucart K, Ionescu AM. Length scaling of the double gate tunnel FET with a high-K gate dielectric. Solid-State Electronics. 2007;**51**(11-12):1500-1507. DOI: 10.1016/j.sse.2007.09.014

[24] Lam K-T, Seah D, Chin S-K, Kumar SB, Samudra G, Yeo Y-C, et al. A simulation study of graphene-nanoribbon tunneling FET with heterojunction channel. IEEE Electron Device Letters. 2010;**31**(6):555-557. DOI: 10.1109/led.2010.2045339

[25] Vishnoi R, Kumar MJ. Compact analytical drain current model of gate-all-around nanowire tunneling FET. IEEE Transactions on Electron Devices. 2014;**61**(7):2599-2603. DOI: 10.1109/ted.2014.2322762

[26] Toh E-H, Wang GH, Chan L, Sylvester D, Heng C-H, Samudra GS, et al. Device design and scalability of a double-gate tunneling field-effect transistor with silicon–germanium source. Japanese Journal of Applied Physics. 2008;**47**(4):2593-2597. DOI: 10.1143/jjap.47.2593

[27] Ahish S, Sharma D, Kumar YBN, Vasantha MH. Performance enhancement of novel InAs/Si hetero double-gate tunnel FET using Gaussian doping. IEEE Transactions on Electron Devices. 2016;**63**(1):288-295. DOI: 10.1109/ted.2015.2503141

[28] Dewey G, Chu-Kung B, Boardman J, Fastenau JM, Kavalieros J, Kotlyar R, et al. Fabrication, characterization, and physics of III–V heterojunction tunneling field effect transistors (H-TFET) for steep sub-threshold swing. In: International Electron Devices Meeting, December 5-7, 2011. Washington, DC: IEEE; 2012. pp. 33.6.1-33.6.4. DOI: 10.1109/iedm.2011.6131666

[29] Bagga N, Dasgupta S. Surface potential and drain current analytical model of gate all around triple metal TFET. IEEE Transactions on Electron Devices. 2017;**64**(2):606-613. DOI: 10.1109/ted.2016.2642165

[30] Bagga N, Sarkar SK. An analytical model for tunnel barrier modulation in triple metal double gate TFET. IEEE Transactions on Electron Devices. 2015;**62**(7):2136-2142. DOI: 10.1109/ted.2015.2434276

[31] Dash S, Mishra G. A new analytical threshold voltage model of cylindrical gate tunnel FET (CG-TFET). Superlattices and Microstructures. 2015;**86**:211-220. DOI: 10.1016/j.spmi.2015.07.049

[32] Lee MJ, Choi WY. Analytical model of single-gate silicon-on-insulator (SOI) tunneling field-effect transistors (TFETs). Solid-State Electronics. 2011;**63**(1):110-114. DOI: 10.1016/j.sse.2011.05.008

[33] Luong G, Strangio S, Tiedemannn A, Lenk S, Trellenkamp S, Bourdelle K, et al. Experimental demonstration of strained Si nanowire GAA n-TFETs and inverter operation with complementary TFET logic at low supply voltages. Solid-State Electronics. 2016;**115**:152-159. DOI: 10.1016/j.sse.2015.08.020

[34] Mookerjea S, Mohata D, Krishnan R, Singh J, Vallett A, Ali A, et al. Experimental demonstration of 100nm channel length In0.53Ga0.47As-based vertical inter-band tunnel field effect transistors (TFETs) for ultra low-power logic and SRAM applications. In: IEEE International Electron Devices Meeting (IEDM), December 7-9, 2009. Baltimore: IEEE; 2010. pp. 1-3. DOI: 10.1109/iedm.2009.5424355

[35] Singh J, Ramakrishnan K, Mookerjea S, Datta S, Vijaykrishnan N, Pradhan D. A novel Si-tunnel FET based SRAM design for ultra low-power 0.3V VDD applications. In: 15th Asia and South Pacific Design Automation Conference (ASP-DAC), January 18-21, 2010. Taipei: IEEE; 2010. pp. 181-186. DOI: 10.1109/aspdac.2010.5419897

[36] Im H, Huang X-J, Gu B, Choi Y-K. A dielectric-modulated field-effect transistor for biosensing. Nature Nanotechnology. 2007;**2**(7):430-434. DOI: 10.1038/nnano.2007.180

[37] Narang R, Saxena M, Gupta RS, Gupta M. Dielectric modulated tunnel field-effect transistor—A biomolecule sensor. IEEE Electron Device Letters. 2012;**33**(2):266-268. DOI: 10.1109/led.2011.2174024

[38] Narang R, Reddy KVS, Saxena M, Gupta RS, Gupta M. A dielectric-modulated tunnel-FET-based biosensor for label-free detection: Analytical modeling study and sensitivity analysis. IEEE Transactions on Electron Devices. 2012;**59**(10):2809-2817. DOI: 10.1109/TED.2012.2208115

[39] Narang R, Saxena M, Gupta RS, Gupta M. Comparative analysis of dielectric-modulated FET. IEEE Transactions on Nanotechnology. 2015;**14**(3):427-435. DOI: 10.1109/TNANO.2015.2396899

[40] Kanungo S, Chattopadhyay S, Gupta PS, Rahaman H. Comparative performance analysis of the dielectrically modulated full-gate and short-gate tunnel FET-based biosensors. IEEE Transactions on Electron Devices. 2015;**62**(3):994-1001. DOI: 10.1109/ted.2015.2390774

[41] Kanungo S, Chattopadhyay S, Gupta PS, Sinha K, Rahaman H. Study and analysis of the effects of SiGe source and pocket-doped channel on sensing performance of dielectrically modulated tunnel FET-based biosensors. IEEE Transactions on Electron Devices. 2016;**63**(6):2589-2596. DOI: 10.1109/ted.2016.2556081

[42] Sarkar D, Banerjee K. Proposal for tunnel-field-effect-transistor as ultra-sensitive and label-free biosensors. Applied Physics Letters. 2012;**100**(14):143108. DOI: 10.1063/1.3698093

[43] Bergveld P. Thirty years of ISFETOLOGY. Sensors and Actuators B: Chemical. 2003;**88**(1): 1-20. DOI: 10.1016/s0925-4005(02)00301-5

[44] Kim C-H, Ahn J-H, Lee K-B, Jung C, Park HG, Choi Y-K. A new sensing metric to reduce data fluctuations in a nanogap-embedded field-effect transistor biosensor. IEEE Transactions on Electron Devices. 2012;**59**(10):2825-2831. DOI: 10.1109/ted.2012.2209650

[45] Abdi DB, Kumar MJ. Dielectric modulated overlapping gate-on-drain tunnel-FET as a label-free biosensor. Superlattices and Microstructures. 2015;**86**:198-202. DOI: 10.1016/j.spmi.2015.07.052

[46] Ahangari Z. Performance assessment of dual material gate dielectric modulated nanowire junctionless MOSFET for ultrasensitive detection of biomolecules. RSC Advances. 2016;**6**(92):89185-89191. DOI: 10.1039/c6ra17361f

[47] Knoch J, Appenzeller J. A novel concept for field-effect transistors – The tunneling carbon nanotube FET. In: 63rd Device Research Conference Digest, DRC 05; June 20-22, 2005. Santa Barbara: IEEE; 2005. pp. 153-156. DOI: 10.1109/drc.2005.1553099

[48] Knoch J, Mantl S, Appenzeller J. Impact of the dimensionality on the performance of tunneling FETs: Bulk versus one-dimensional devices. Solid-State Electronics. 2007;**51**(4):572-578. DOI: 10.1016/j.sse.2007.02.001

[49] Wang C, Wu C, Wang J, Huang Q, Huang R. Analytical current model of tunneling field-effect transistor considering the impacts of both gate and drain voltages on tunneling. Science China Information Sciences. 2014;**58**(2):1-8. DOI: 10.1007/s11432-014-5196-3

[50] Synopsys. Sentaurus Device User Guide. Mountain View: Synopsys, Inc.; 2011

[51] Ortiz-Conde A, García S Fj, Liou J, Cerdeira A, Estrada M, Yue Y. A review of recent MOSFET threshold voltage extraction methods. Microelectronics Reliability. 2002;**42**(4-5):583-596. DOI: 10.1016/s0026-2714(02)00027-6

[52] Ortiz-Conde A, García-Sánchez FJ, Muci J, Barrios AT, Liou JJ, Ho C-S. Revisiting MOSFET threshold voltage extraction methods. Microelectronics Reliability. 2013;**53**(1):90-104. DOI: 10.1016/j.microrel.2012.09.015

[53] Goswami R, Bhowmick B, Baishya S. Electrical noise in circular gate tunnel FET in presence of interface traps. Superlattices and Microstructures. 2015;**86**:342-354. DOI: 10.1016/j.spmi.2015.07.064

[54] Tsividis Y. Operation and Modelling of the MOS Transistor. 2nd ed. New York: Oxford University Press; 1999

[55] Singh S, Kondekar P, Jaiswal NK. Label-free biosensor using nanogap embedded dielectric modulated schottky tunneling source impact ionization MOS. Microelectronic Engineering. 2016;**149**:129-134. DOI: 10.1016/j.mee.2015.10.005

IntechOpen